

RESEARCH ARTICLE

Open Access



Chitosan oligosaccharide inhibits skull resorption induced by lipopolysaccharides in mice

Ke Guo¹, Zong Lin Liu¹, Wen Chao Wang¹, Wei Feng Xu¹, Shi Qi Yu^{2*} and Shan Yong Zhang^{1*}

Abstract

Background: Low-molecular-weight chitosan oligosaccharide (LMCOS), a chitosan degradation product, is water-soluble and easily absorbable, rendering it a popular biomaterial to study. However, its effect on bone remodelling remains unknown. Therefore, we evaluated the effect of LMCOS on lipopolysaccharide (LPS)-induced bone resorption in mice.

Methods: Six-week-old male C57BL/6 mice (n = five per group) were randomly divided into five groups: PBS, LPS, LPS + 0.005% LMCOS, LPS + 0.05% LMCOS, and LPS + 0.5% LMCOS. Then, the corresponding reagents (300 μ L) were injected into the skull of the mice. To induce bone resorption, LPS was administered at 10 mg/kg per injection. The mice were injected three times a week with PBS alone or LPS without or with LMCOS and sacrificed 2 weeks later. The skull was removed for micro-computed tomography, haematoxylin-eosin staining, and tartrate-resistant acid phosphatase staining. The area of bone damage and osteoclast formation were evaluated and recorded.

Results: LMCOS treatment during LPS-induced skull resorption led to a notable reduction in the area of bone destruction; we observed a dose-dependent decrease in the area of bone destruction and number of osteoclasts with increasing LMCOS concentration.

Conclusions: Our findings showed that LMCOS could inhibit skull bone damage induced by LPS in mice, further research to investigate its therapeutic potential for treating osteolytic diseases is required.

Keywords: Chitosan oligosaccharide, LPS, Micro-CT, TRAP staining, Bone resorption

Background

Chitosan oligosaccharide (COS) is a product of chitosan degradation. Chitin is the second largest biological macromolecule polysaccharide in nature, and chitosan is the product of chitin deacetylation. Chitosan is a non-toxic biocompatible molecule that possesses antibacterial properties and promotes the growth of osteoblasts, cell proliferation, and differentiation [1–4]. Chitosan is an integral component of a new type of mixed biofilm particularly pertaining to the field of guided tissue regeneration (GTR) and guided bone regeneration (GBR) [5, 6]. In the field of bone-defect scaffold materials, a chitosan

composite porous scaffold was shown to have better porosity and osteogenic activity with higher bone formation volume and rate than the conventional bone scaffold material, making it a promising new material for repairing bone defects [7]. Although the use of chitosan in GBR, GTR, and bone defect scaffold applications has been widely reported, it has certain disadvantages, such as its large molecular weight, water insolubility, low degradation rate, and relatively slow absorption rate. In contrast, COS, which is the product of chitosan degradation, has a low molecular weight and is water-soluble and easily absorbed, rendering it a popular biomaterial to study in recent years.

COS has been widely used in agriculture, industry, biomedical biomaterials, food bioengineering, and other fields for several decades. Several studies have also suggested COS inhibits apoptosis and promotes the healing

* Correspondence: 976748974@qq.com; zhangshanyong@126.com

²Shanghai Ninth People's Hospital, School of Biomedical Engineering, Shanghai Jiao Tong University, Shanghai, China

¹Department of Oral Surgery, Shanghai Ninth People's Hospital, College of Stomatology, Shanghai Jiao Tong University School of Medicine; Shanghai Key Laboratory of Stomatology, 639 ZhiZaoJu Road, Shanghai 200011, China



of bone defects [8–11]. COS is also reported to promote the proliferation and differentiation of osteoblasts, and the expression of genes related to bone defects [12, 13]. Nevertheless, the effect of low-molecular-weight chitosan oligosaccharide (LMCOS) on bone remodelling has not been reported. In this study, we evaluated the effect of LMCOS on inflammatory bone destruction induced by lipopolysaccharide (LPS) in mice. We established an inflammatory bone destruction model and treated the mice with different concentrations of LMCOS.

Methods

Materials and equipment

Six-week-old male C57BL/6 mice were from Shanghai West Poole-Baykay Laboratory Animal Co., Ltd. (Shanghai, China); bacterial LPS and a tartrate-resistant acid phosphatase (TRAP) detection kit were purchased from Sigma-Aldrich (St. Louis, MO, USA); chitosan oligosaccharide powder (polymerization degree, 2–10; average molecular weight, 1000 Da; purity, >98%; deacetylation degree, 99%). The micro-CT scanner (μ CT-100) used in this study was purchased from Scanco Medical AG, Brüttisellen, Switzerland. This study was approved by the Ethics Committee of Shanghai Ninth People's Hospital (SH9H-2019-A502–1).

Inflammatory bone destruction model and LMCOS treatment

LPS was dissolved in phosphate-buffered saline (PBS) at a concentration of 1 g/L. The LPS bone destruction model was described previously; briefly, bone destruction was induced by injecting LPS between the subcutaneous tissue and bone periosteum of the head in mice [14]. The mice were randomly divided into five groups ($n =$ five per group): control mice injected with PBS only (300 μ L); mice injected with LPS (200 μ L) and PBS (100 μ L); mice injected with LPS (200 μ L) and 0.005% LMCOS (100 μ L); mice injected with LPS (200 μ L) and 0.05% LMCOS (100 μ L); mice injected with LPS (200 μ L) and 0.5% LMCOS (100 μ L). The mice were injected three times per week and euthanized 2 weeks later. To reduce pain for euthanasia, the mice were briefly anaesthetized in an isoflurane-filled box to induce early unconsciousness, and then the mice were killed with cervical dislocation.

Micro-computed tomography

The cranium of each mouse was harvested, and the soft tissue around the bone was separated for micro-computed tomography (micro-CT). The scanning parameters were 70 kV, 114 mA, and a scanning thickness of 50 μ m. A bone mass analysis was performed to evaluate bone damage quantitatively after three-dimensional reconstruction.

Haematoxylin and eosin (H&E) staining

The calvarial bone tissue of each mouse was fixed in 4% paraformaldehyde for 24 h and then washed overnight. Subsequently, the tissue was decalcified with 10% EDTA at 4 °C, dehydrated by a graded series of ethanol, and embedded in paraffin after *n*-butyl alcohol exchanges. Each specimen was sectioned to a near-far-median sagittal section thickness of 4 μ m. Following sectioning, H&E staining was performed to visualize cranial cap bone defects under a microscope.

TRAP staining

The TRAP stain was prepared according to the manufacturer's instructions. Calvarial bone specimens were deparaffinized with dimethylbenzene and processed with a graded series of ethanol concentrations. The TRAP stain was then applied to the tissues and incubated at 37 °C for 1 h. Subsequently, the tissues were re-stained with haematoxylin for 2 min, cleared with xylene, and mounted and sealed with neutral gum. The tissue slides were observed under an optical microscope, and TRAP-positive cells (brown) were counted and subjected to statistical analysis.

Statistical analysis

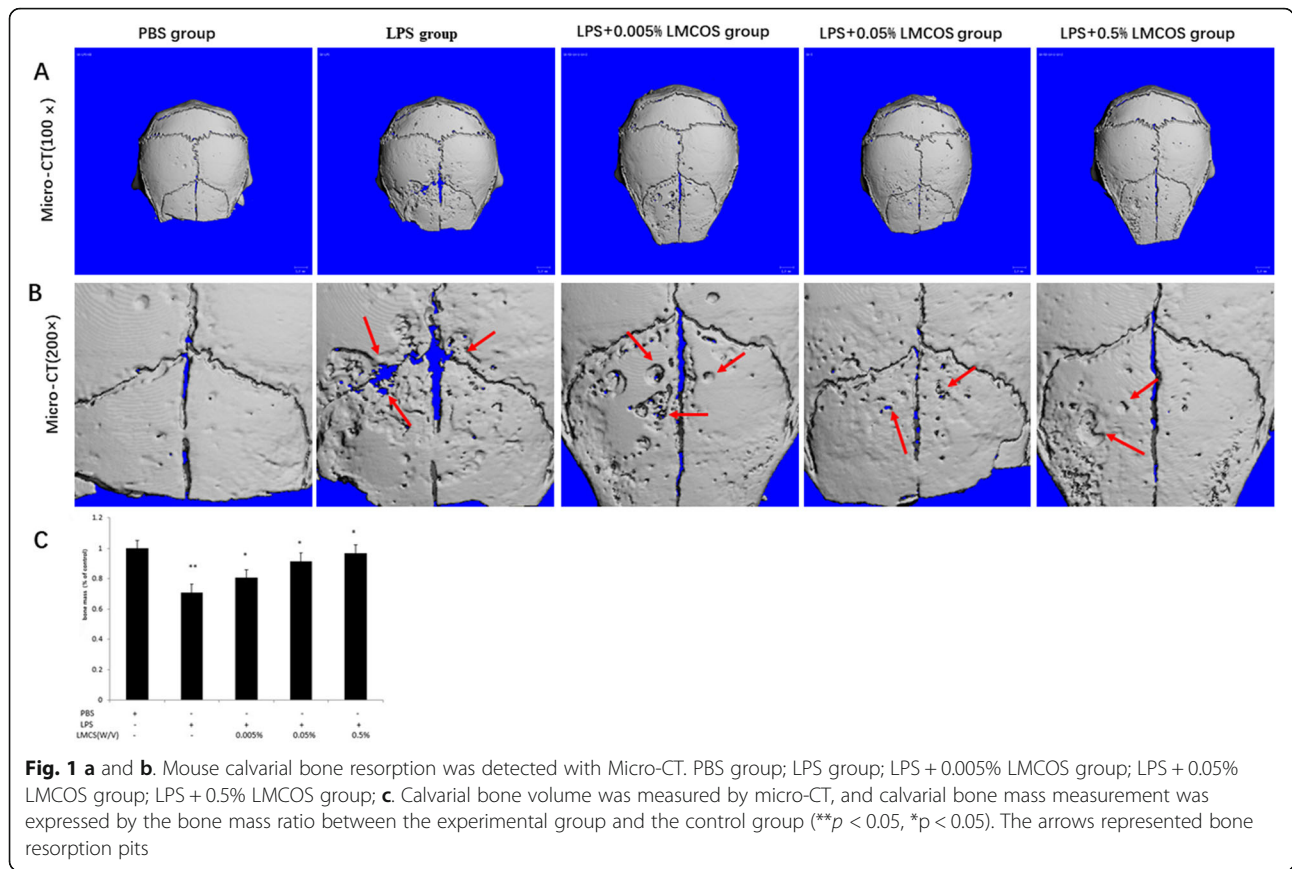
The data are presented as the mean \pm standard deviation, and statistical analysis was performed using the SPSS 21.0 software package (IBM, Armonk, NY, USA). A single factor analysis of variance and Student-Newman-Keuls (SNK) test were used for the statistical analysis. A *P*-value < 0.05 indicated a significant difference between groups.

Results

LMCOS decreases the formation of bone resorption pits induced by LPS

The formation of cranial resorption pits was assessed using micro-CT. Compared with the PBS-only control group, the formation of cranial resorption pits was more apparent in the LPS group (Fig. 1a and b). However, LPS-induced bone resorption pits were significantly reduced in mice treated with LMCOS compared with the LPS treated group, and the bone resorption pits were reduced further with increasing LMCOS concentrations (Fig. 1a and b).

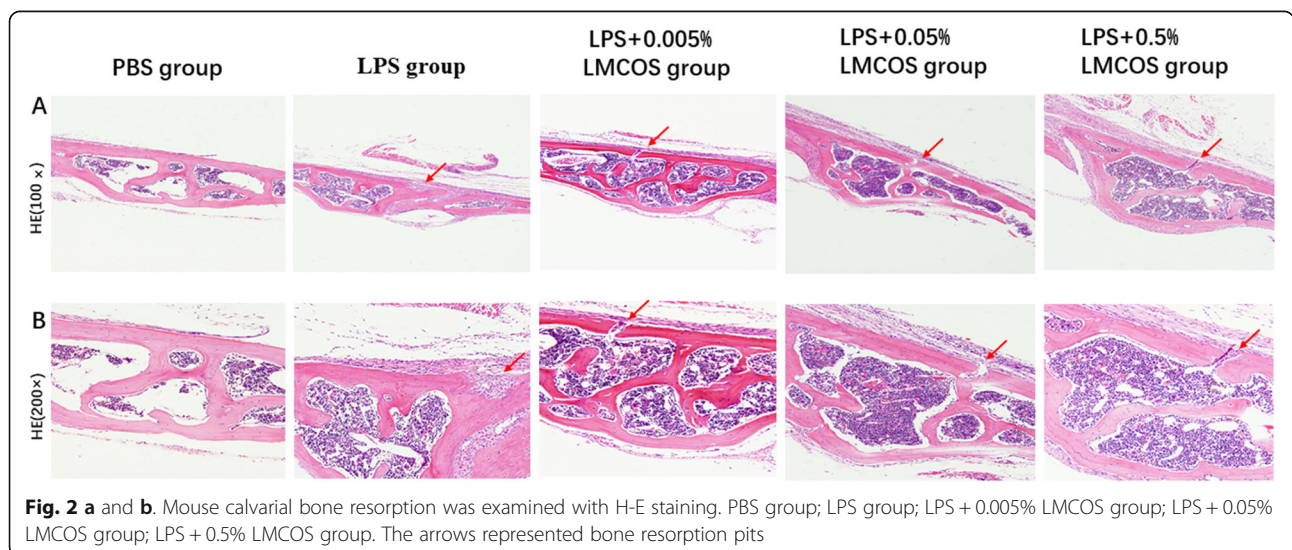
The statistical analysis of the micro-CT scans of the skull caps of mice showed that the skull bone mass of mice in the LPS group was reduced compared with that of mice in the blank control group. The bone mass of the LPS + 0.005% LMCOS group, LPS + 0.05% LMCOS group, and LPS + 0.5% LMCOS group was higher than that of the LPS group. Furthermore, the number of bone trabeculae was higher in the high-dose group than in the low-dose group. Compared with the LMCOS group, the



PBS group and LPS group exhibited statistically significant differences. At the same time, bone indexes such as bone resorption cavities, bone trabeculae thickness, and number showed that the high-concentration LMCOS group had stronger inhibiting effects on bone resorption than that of the low concentration LMCOS group (Fig. 1c) (** $p < 0.05$, * $p < 0.05$).

LMCOS limits LPS-induced cranial bone damage

The H&E staining results showed that the cranium of LPS-treated mice was notably damaged compared with that of mice in the PBS control group (Fig. 2a and b). However, in mice treated with LMCOS, the cranial damage induced by LPS was significantly inhibited, and bone resorption was significantly reduced. The bone damage



was further decreased by increasing concentrations of LMCOS (Fig. 2a and b).

LMCOS reduces the number of TRAP-positive cells

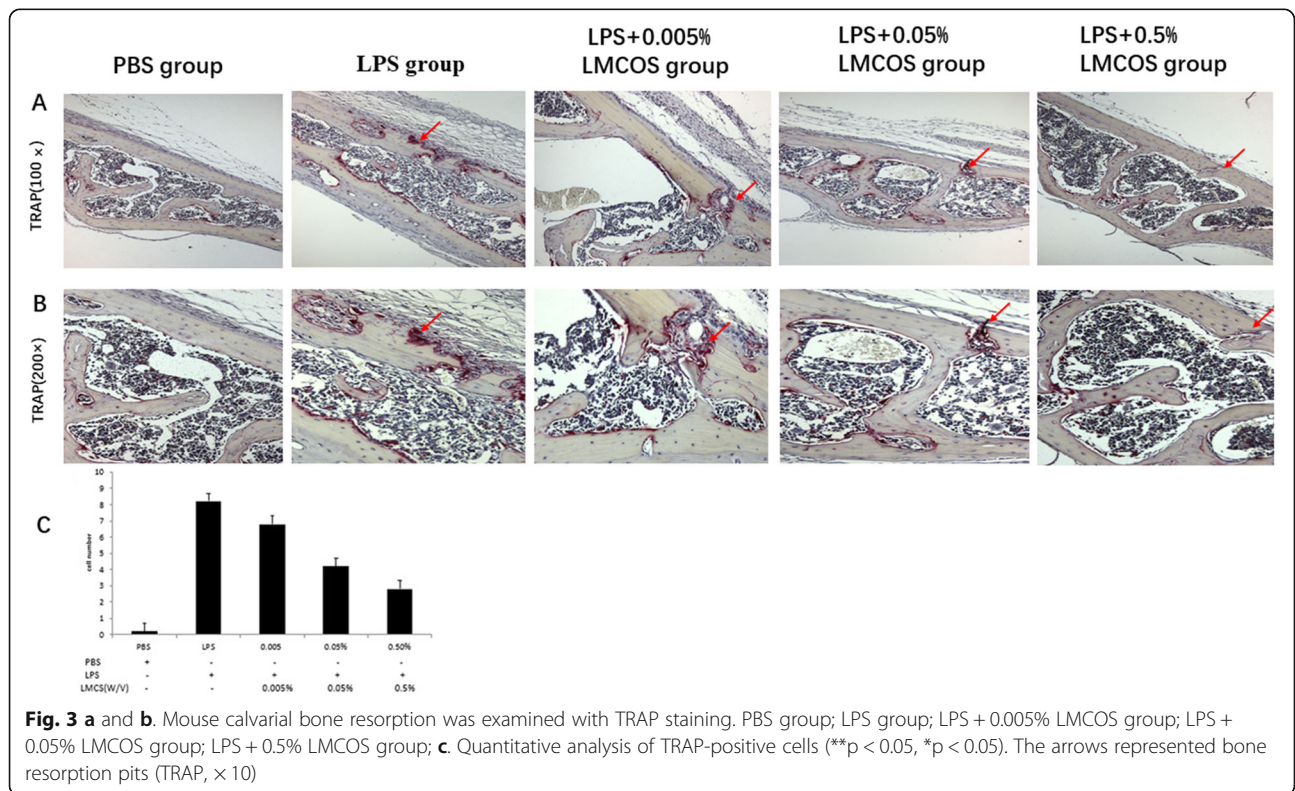
The TRAP staining showed that LMCOS inhibited osteoclastogenesis induced by LPS (Fig. 3a and b). The number of TRAP-positive cells was graphed and subjected to statistical analysis (Fig. 3c). The number of osteoclasts increased in the LPS group compared with the control group. At the same time, the number of osteoclasts in the LPS + 0.005% LMCOS group, LPS + 0.05% LMCOS group, and LPS + 0.5% LMCOS group was lower than that in the LPS group alone. The number of osteoclasts in the high-dose group was less than that in the low-dose group. Compared with the LMCOS group, the PBS group and LPS group exhibited statistically significant differences. In the processing of osteoclasts, the group with a high concentration of LMCOS exhibited stronger inhibitory effects on bone resorption than that of the group with a low concentration of LMCOS. LMCOS treatment significantly reduced the number of TRAP-positive cells induced by LPS.

Discussion

In GBR, GTR, and related technologies, bone healing materials remain the most critical components of the technologies. Currently, the main clinical applications of GBR and GTR include autogenous bone [15], heterogeneous

bone [16], allogeneic bone [17–19], and artificial synthetic materials [20]. The ideal bone healing materials should possess the following characteristics: 1) biocompatibility and non-toxicity; 2) biodegradability and absorbency; 3) a biological activity that simulates the structure of the bone matrix and promotes the regeneration of bone tissue [21].

In recent years, numerous studies have shown that chitin, chitosan, COS, and their derivatives also have certain effects on in vitro cultured cells, mainly to promote cell proliferation and differentiation. The osteogenic properties of these materials in bone defect reconstruction have also been evaluated in several studies [22, 23]. A new chitosan composite porous scaffold has been studied and entered the application stage. Chitosan-composite porous stent, a new material for repairing bone defects, has better porosity and good osteogenic activity, with bone formation volume and bone formation rate superior to those of conventional bone scaffold materials [24]. However, its large molecular weight, water insolubility, low degradation rate, and relatively slow absorption rate have restricted its applications in medicine. As a degradation product of chitosan, LMCOS has the advantages of low molecular weight, biocompatibility, biodegradability, antibacterial properties, and absorbability [25]. Compared with chitosan, LMCOS has an improved degradation rate and solubility. Furthermore, studies have shown that LMCOS can promote osteoblast proliferation [4]. Nevertheless, the



role of LMCOS in inhibiting osteoclasts is yet to be determined.

Results of our preliminary study provided early evidence of the LMCOS effect on osteoclasts, indicating its inhibitory effect on the osteoclast process. To further explore the ability of LMCOS to inhibit the osteoclast process, we utilized a mouse LPS-induced cranial bone destruction model to evaluate the effect of LMCOS on inflammatory bone damage [26]. LPS induces mononuclear macrophages to secrete a variety of inflammatory mediators and promote the fusion of osteoclast precursors, maintains mature osteoclast activity, and stimulates osteoclasts to perform bone resorption functions [27]. We tested different concentrations of LMCOS in an experimental animal model to assess its dose-dependent inhibition of the osteoclast process. Using micro-CT scanning, we verified that LPS induced significant cranial bone resorption; however, LMCOS was able to reduce bone resorption lacunae in a dose-dependent manner. Results of the H&E staining also showed that LMCOS could significantly inhibit bone damage induced by LPS. TRAP staining further confirmed that the number of osteoclasts was decreased with LMCOS intervention compared with that in mice injected with LPS only. Therefore, our findings indicated that LMCOS limits LPS-induced bone destruction by inhibiting osteoclast formation.

Conclusions

In summary, our study demonstrated the ability of LMCOS to inhibit skull bone destruction induced by LPS in mice. Our findings suggested the therapeutic application of LMCOS for treating bone diseases, although the specific molecular mechanism needs further studies.

Abbreviations

COS: Chitosan oligosaccharide; GBR: Guided bone regeneration; GTR: Guided tissue regeneration; LMCOS: Low-molecular-weight chitosan oligosaccharide; LPS: Lipopolysaccharide; micro-CT: micro-computed tomography; PBS: Phosphate-buffered saline; TRAP: Tartrate-resistant acid phosphatase

Acknowledgments

Not Applicable.

Authors' contributions

All authors have contributed significantly to this work and contributed to the paper in equal parts. KG had the idea for the research and developed the concept, participated in the experiments on animals, literature research, writing the manuscript and carried out proofreading. ZLL joined in experiments on animals, WCW joined in the acquisition of data. WFX took part in analysis of data, SQY and SYZ participated in study development, literature research, writing of the manuscript and carried out proofreading. All authors have read and approved the manuscript and ensure that this is the case.

Funding

It was supported by the National Natural Science Foundation of China in 2017 (81671010), including the design of the study and collection, analysis, and interpretation of data and writing the manuscript. Specially, this project

offered the financial supports included the purchases of animals, reagents for HE, Trap staining, and Micro-CT analysis.

Availability of data and materials

The dataset used and/or analyzed during the current study are available from the corresponding author on reasonable request.

Ethics approval and consent to participate

The study design was approved by the Ethical Committee of Shanghai Ninth People's Hospital. The registration number is SH9H-2019-A502-1.

Consent for publication

Not applicable.

Competing interests

The authors declare that they have no competing interests.

Received: 1 September 2019 Accepted: 5 November 2019

Published online: 27 November 2019

References

- Wieckiewicz M, Boening KW, Grychowska N, et al. Clinical application of chitosan in dental specialties [J]. *Mini Rev Med Chem*. 2017;17(5):401–9.
- Ramasamy P, Subhadrappa N, Thinesh T, et al. Characterization of bioactive chitosan and sulfated chitosan from *Doryteuthis singhalensis*, (Ortmann, 1891) [J]. *Int J Biol Macromol*. 2017;99(2):682–91.
- Khodaghali F, Eftekhazadeh B, Maghsoudi N, et al. Chitosan prevents oxidative stress-induced amyloid β formation and cytotoxicity in NT2 neurons: involvement of transcription factors Nrf2 and NF- κ B [J]. *Mol Cell Biochem*. 2010;337(1–2):39–51.
- Costa -Pinto AR, Correlo VM, Sol PC, et al. Osteogenic differentiation of human bone marrow mesenchymal stem cells seeded on melt based chitosan scaffolds for bone tissue engineering applications [J]. *Biomacromolecules*. 2009;10(8):2067–73.
- Teng SH, Lee EJ, Wang P, et al. Three-layered membranes of collagen/hydroxyapatite and chitosan for guided bone regeneration [J]. *J Biomed Mater Res B*. 2010;87B(1):132–8.
- Zhou T, Liu X, Sui B, et al. Development of fish collagen/bioactive glass/chitosan composite nanofibers as a GTR/GBR membrane for inducing periodontal tissue regeneration. [J]. *Biomed Mater*. 2017;12(5):055004.
- Kumar JP, Lakshmi L, Jyothisna V, et al. Synthesis and characterization of diopside particles and their suitability along with chitosan matrix for bone tissue engineering in vitro and in vivo [J]. *J Biomed Nanotechnol*. 2014; 10(6):970–81.
- Li J, He J, Yu C. Chitosan oligosaccharide inhibits LPS-induced apoptosis of vascular, endothelial cells through the BK Ca channel and the p38 signaling pathway [J]. *Int J Mol Med*. 2012;30(1):157–64.
- Xu Q, Wang W, Yang W, et al. Chitosan oligosaccharide inhibits EGF-induced cell growth possibly through blockade of epidermal growth factor receptor/mitogen-activated protein kinase pathway [J]. *Int J Biol Macromol*. 2017;98:502–5.
- Muanprasat C, Chatsudhipong V. Chitosan oligosaccharide: biological activities and potential therapeutic applications [J]. *Pharmacol Ther*. 2017; 170(5):80–97.
- Zhang C, Ling Y, Yan Z, et al. Chitosan oligosaccharides inhibit IL-1 β -induced chondrocyte apoptosis via the P38 MAPK signaling pathway [J]. *Glycoconj J*. 2016;33(5):1–10.
- Dang Y, Li S, Wang W, et al. The effects of chitosan oligosaccharide on the activation of murine spleen CD11c⁺ dendritic cells via toll-like receptor 4 [J]. *Carbohydr Polym*. 2011;83(3):1075–81.
- Juthamas R, Sorada K, Yasuhiko T, et al. Growth and osteogenic differentiation of adipose-derived and bone marrow-derived stem cells on chitosan and chitooligosaccharide films [J]. *Carbohydr Polym*. 2009;78(4): 873–8.
- Pelegri AA, da Costa CE, Correa ME, et al. Clinical and histomorphometric evaluation of extraction sockets treated with an autologous bone marrow graft [J]. *Clin Oral Implants Res*. 2010;21(5):535–42.
- Khalifa AK, Wada M, Ikebe K, et al. To what extent residual alveolar ridge can be preserved by implant? A systematic review [J]. *Int J Implant Dent*. 2016; 2(1):22–30.

16. Kresnoadi U, Ariani MD, Djulaeha E, et al. The potential of mangosteen (*Garcinia mangostana*) peel extract, combined with demineralized freeze-dried bovine bone xenograft, to reduce ridge resorption and alveolar bone regeneration in preserving the tooth extraction socket [J]. *J Indian Prosthodont Soc.* 2017;17(3):282–8.
17. Rasperini G, Canullo L, Dellavia C, et al. Socket grafting in the posterior maxilla reduces the need for sinus augmentation [J]. *Int J Periodontics Restorative Dent.* 2010;30(3):265–73.
18. Maiorana C, Poli PP, Deflorian M, et al. Alveolar socket preservation with demineralised bovine bone mineral and a collagen matrix [J]. *J Periodontal Implant Sci.* 2017;47(4):194–210.
19. Mayer Y, Zigdon-Giladi H, Machtei EE. Ridge preservation using composite alloplastic materials: a randomized control clinical and histological study in humans [J]. *Clin Implant Dent Relat Res.* 2016;18(6):1163–70.
20. Wang YF, Wang CY, Wan P, et al. Comparison of bone regeneration in alveolar bone of dogs on mineralized collagen grafts with two composition ratios of nano-hydroxyapatite and collagen [J]. *Regen Biomater.* 2016;3(1):33–40.
21. Li L, Khansari A, Shapira L, et al. Contribution of interleukin-11 and prostaglandin(s) in lipopolysaccharide-induced bone resorption in vivo [J]. *Infect Immun.* 2002;70(7):3915–22.
22. Jayash SN, Hashim NM, Misran M, et al. Formulation and in vitro and in vivo evaluation of a new osteoprotegerin-chitosan gel for bone tissue regeneration [J]. *J Biomed Mater Res A.* 2017;105(2):398–407.
23. Ruan SQ, Deng J, Yan L, et al. Composite scaffolds loaded with bone mesenchymal stem cells promote the repair of radial bone defects in rabbit model. [J]. *Biomed Pharmacother.* 2017;97(2):600–6.
24. Kumar JP, Lakshmi L, Jyothisna V, et al. Synthesis and characterization of diopside particles and their suitability along with chitosan matrix for bone tissue engineering in vitro and in vivo [J]. *J Biomed Nanotechnol.* 2014; 10(6):970–81.
25. Teng SH, Lee EJ, Wang P, et al. Three -layered membranes of collagen/ hydroxyapatite and chitosan for guided bone regeneration [J]. *J Biomed Mater Res B Appl Biomater.* 2008;87(1):132–8.
26. Guo J, Yang D, Okamura H, et al. Calcium hydroxide suppresses *Porphyromonas endodontalis* lipopolysaccharide-induced bone destruction [J]. *J Dent Res.* 2014;93(5):508–13.
27. Cao JJ, Gregoire BR, Shen CL. A high-fat diet decreases bone mass in growing mice with systemic chronic inflammation induced by low-dose, slow-release lipopolysaccharide pellets [J]. *J Nutr.* 2017;147(10):1909–16.

Publisher's Note

Springer Nature remains neutral with regard to jurisdictional claims in published maps and institutional affiliations.

Ready to submit your research? Choose BMC and benefit from:

- fast, convenient online submission
- thorough peer review by experienced researchers in your field
- rapid publication on acceptance
- support for research data, including large and complex data types
- gold Open Access which fosters wider collaboration and increased citations
- maximum visibility for your research: over 100M website views per year

At BMC, research is always in progress.

Learn more biomedcentral.com/submissions

